Sensor Reduction for Driver-Automation Shared Steering Control via an Adaptive Authority Allocation Strategy

Tran Anh-Tu Nguyen, Chouki Sentouh, Jean-Christophe Popieul

Sensor Reduction for Driver–Automation Shared Steering Control via an Adaptive Authority Allocation Strategy

Article *in* IEEE/ASME Transactions on Mechatronics · February 2018

DOI: 10.1109/TMECH.2017.2698216

CITATIONS
103

READS
530

3 authors, including:

Anh-Tu Nguyen
Université Polytechnique Hauts-de-France
140 PUBLICATIONS **2,084** CITATIONS

SEE PROFILE

Chouki Sentouh
LAMIH UMR CNRS 8201 Hauts-de-France Polytechnic University
114 PUBLICATIONS **2,057** CITATIONS

SEE PROFILE

Sensor Reduction for Driver-Automation Shared Steering Control via an Adaptive Authority Allocation Strategy

Anh-Tu Nguyen, Chouki Sentouh and Jean-Christophe Popieul

***Abstract*—This paper presents a new shared control method for lane keeping assist (LKA) systems of intelligent vehicles. The proposed method allows the LKA system to effectively share the control authority with a human driver by avoiding or minimizing the conflict situations between these two driving actors. To realize the shared control scheme, the *unpredictable* driver-automation interaction is explicitly taken into account in the control design via a *fictive* driver activity variable. This latter is judiciously introduced into the driver-road-vehicle system to represent the driver's need for assistance in accordance with his/her real-time driving activity. Using Lyapunov stability arguments, Takagi-Sugeno fuzzy model-based design conditions are derived to handle not only the time-varying driver activity variable but also a large variation range of vehicle speed. Both simulation and hardware experiments are presented to demonstrate that the proposed control strategy together with an LMI (linear matrix inequality) design formulation provide an effective tool to deal with the challenging shared steering control issue. In particular, a fuzzy output feedback control scheme is exploited to achieve the shared control goal without at least two important vehicle sensors. These physical sensors are widely employed in previous works to measure the lateral speed and the steering rate for the control design and real-time implementation. The successful results of this idea of sensor-reduction control has an obvious interest from practical viewpoint.**

***Index Terms*—Lane keeping assist system, shared control, human-in-the-loop control, fuzzy model-based control, Lyapunov method, vehicle lateral control.**

I. Introduction

THE automobile has been one of the most important products of the twentieth century which has generated an immense industry. However, driving is a *dangerous* activity and the damages caused by road accidents have serious consequences for individuals and the society. The failure of human drivers' performance (e.g. inattention, illness, drowsiness) remains one of the most important causes of accidents [1]. This has greatly motivated the research effort from both academic and industrial settings to develop advanced assistance systems to help the driver in various circumstances [2], [3]. In particular, a large body of literature has been recently devoted to the vehicle lateral control, see [4]–[6] and references therein.

From the viewpoint of human-machine interaction, the introduction of a driver steering assistance system into a vehicle can modify the real-time driving activity of the driver and also the risks from the external environment [1]. This naturally leads to the conflict issue between the human driver and the automation in many driving situations. Therefore, the human-automation interaction is considered as the most challenging part in the control design procedure of such assistance systems [2]. Recently, shared control approach has been appeared as a promising solution to deal with this issue [7], [8]. Shared control refers to a control scheme in which there is a combination of a human input and a feedback control function. The control goal is to guarantee that the designed assistance actions do not prevent the human operator to perform some specific tasks that have not been detected by the automation, or even better, the automation should assist him/her to realize these maneuvers. To achieve this goal, an active coordination of control authority between the human driver and the automation is required [9]. Existing works in the framework of the vehicle shared steering control [4], [10] have also shown that the integration of driver's behaviors into the control loop (via measurements and modeling) contributes to improve the conflict management.

This paper discusses the design of shared controllers for lane keeping assist (LKA) systems of intelligent vehicles. Up to now, shared steering control which can *adaptively* modify the control authority allocation between the human driver and the LKA system according to the driving conditions still remains open [5], [7]. Based on an $\mathcal{H}_2-$preview optimization problem, a shared controller has been presented for only lane keeping task in [4]. A fuzzy-based shared controller for both lane keeping and obstacle avoidance has been also proposed in [10]. It should be stressed that the shared controllers in both [4] and [10] exploit neither the real-time driving activity nor the driving state of human drivers provided by the supervision level to manage the conflict issue. An MPC (model predictive control) framework for shared control has been recently presented in [6], where the control objective of matching the driver's steering action is conflicting to other ones such as vehicle stability and obstacle avoidance. In particular, the ultimate control authority is always allocated to the automated system, and the driver cannot overrule it. To overcome the above drawbacks, we have proposed to introduce

Manuscript received September 17, 2016; revised January 18, 2017; accepted April 05, 2017. This work has been done within the framework of the CoCoVeA project (ANR-13-TDMO-0005), funded by the Agence Nationale de la Recherche. This work was also supported by the International Campus on Safety and Intermodality in Transportation, the Hauts-de-France Region, the European Community, the Regional Delegation for Research and Technology, the Ministry of Higher Education and Research, and the French National Center for Scientific Research.

A.-T. Nguyen, C. Sentouh and J.-C. Popieul are with the Control Department of the laboratory LAMIH UMR CNRS 8201, University of Valenciennes, France (e-mails: nguyen.trananhtu@gmail.com, {chouki.sentouh, jean-christophe.popieul}@univ-valenciennes.fr).

a *fictive* variable into the driver-road-vehicle system [5]. This variable, representing the real-time driving information of the human driver, is *explicitly* considered in the control design to manage effectively the conflict between two driving actors.

Over the years, fuzzy model-based control has been extensively investigated to deal with complex nonlinear systems, see [11]–[13] and references therein. This is mainly due to the following reasons. First, fuzzy systems have universal approximation capability for any smooth nonlinear function. Recently, this outstanding feature has been effectively exploited in [12] (respectively in [14]) to handle the unmodeled dynamics for the design of an adaptive fuzzy backstepping controller of nonlinear systems (respectively nonlinear time-delay systems). Second, based on the use of Takagi-Sugeno (T-S) fuzzy models [11], stability analysis and control design of nonlinear systems can be recast as LMI (linear matrix inequality) optimization problems, which are effectively solved with numerical solvers [15]. Moreover, fuzzy control methods have been successfully applied to numerous real-world applications [5], [16], [17].

Motivated by the above issues, we propose a new fuzzy model-based shared controller for LKA systems. The main features of this paper are summarized as follows. (1) The proposed shared controller is based on the adaptive control authority allocation strategy proposed in [5] to deal with the driver-automation interaction. Hence, this controller can provide an *appropriate* assistance in accordance with the real-time driving activity of the driver and the driving situations. (2) T-S model-based control is used to handle the time-varying nature of both vehicle speed and the introduced driver activity variable. Note that considering the speed variation into the design procedure is crucial to guarantee not only a good control performance but also a better human-machine coordination under various driving situations [10]. However, this has been mostly neglected in the literature of vehicle lateral control to simplify the design task [4], [6]. (3) In this paper, the measurements of the lateral speed and the steering rate are assumed to be *unavailable* due to cost reasons of the corresponding sensors[1]. State-feedback control schemes *cannot* be applied to this situation as most of related works in the control framework of intelligent vehicles [4], [5], [10]. To this end, based on a fuzzy output feedback scheme and an LMI formulation, we propose a *sensor reduction* control method for LKA systems. By "sensor reduction", it means that the designed controller can achieve the shared control goal even if the number of feedback sensors is reduced from six to four. (4) Both simulation and experimental results are presented to demonstrate the effectiveness of the proposed shared control methodology. To the best of our knowledge, experimental results of driver-automation shared control with only *partial* information on the vehicle states have not been reported in the open literature.

This paper extends our preliminary results in [18], provides formal proofs of all technical statements. In particular, experimental results conducted with a human driver and an advanced interactive driving simulator are also included. The paper is organized as follows. Section II presents the modeling of the driver-road-vehicle system. The proposed shared steering control method is discussed in Section III. In Section IV, the development of a T-S fuzzy output feedback controller is presented, and followed by its application to the control design of the studied LKA system. Both numerical simulation and real-time validation results are given in Section V to verify the practical performance of the proposed methodology. Finally, Section VI concludes the paper.

[1]For example, the cost of a CORREVIT optical sensor used to measure the lateral speed is about 15k€.

II. Driver-Vehicle Modeling for Shared Steering Control of Lane Keeping Assist Systems

This section presents the modeling of the driver-road-vehicle system used for lateral control purposes. The vehicle parameters and notations are given in Table I.

A. Road-Vehicle Model

Since we focus on the shared steering control, the bicycle model [19] is used here to represent the vehicle lateral dynamics, see Fig. 1. Then, the road-vehicle model integrating the electric power steering system is described by [4], [10]:

$$\dot{x}_v = Ax_v + B(T_c + T_d) + B_w w \tag{1}$$

where the vector $x_v^\top = \begin{bmatrix} v_y & r & \psi_L & y_L & \delta & \dot{\delta} \end{bmatrix}$ is composed of the lateral velocity v_y, the yaw rate r, the heading error ψ_L, the lateral offset y_L from the road centerline at a look-ahead distance l_s, the steering angle δ and its time derivative $\dot{\delta}$. For system (1), the driver torque T_d is measured whereas the assistance torque T_c has to be designed to manage effectively the human-automation conflict issue. The lateral wind force f_w and the road curvature ρ_r are system disturbances, i.e. $w^\top = \begin{bmatrix} f_w & \rho_r \end{bmatrix}$. The system matrices are given as follows:

$$A = \begin{bmatrix} a_{11} & a_{12} & 0 & 0 & b_1 & 0 \\ a_{21} & a_{22} & 0 & 0 & b_2 & 0 \\ 0 & 1 & 0 & 0 & 0 & 0 \\ 1 & l_s & v_x & 0 & 0 & 0 \\ 0 & 0 & 0 & 0 & 0 & 1 \\ T_{s_1} & T_{s_2} & 0 & 0 & T_{s_3} & T_{s_4} \end{bmatrix}, \quad B_w = \begin{bmatrix} e_1 & 0 \\ e_2 & 0 \\ 0 & -v_x \\ 0 & 0 \\ 0 & 0 \\ 0 & 0 \end{bmatrix},$$

$$B = \begin{bmatrix} 0 & 0 & 0 & 0 & 0 & \rho \end{bmatrix}^\top,$$

where

$$a_{11} = \frac{-2(C_r + C_f)}{Mv_x}, \quad a_{12} = \frac{2(l_r C_r - l_f C_f)}{Mv_x} - v_x,$$
$$a_{21} = \frac{2(l_r C_r - l_f C_f)}{I_z v_x}, \quad a_{22} = \frac{-2(l_r^2 C_r + l_f^2 C_f)}{I_z v_x},$$
$$T_{s1} = \frac{2K_p C_f \eta_t}{I_s R_s^2 v_x}, \quad T_{s2} = \frac{2K_p C_f l_f \eta_t}{I_s R_s^2 v_x}, \quad \rho = \frac{1}{I_s R_s},$$
$$T_{s3} = \frac{-2K_p C_f \eta_t}{I_s R_s^2}, \quad T_{s4} = \frac{-Bs}{I_s}, \quad b_1 = \frac{2C_f}{M},$$
$$b_2 = \frac{2l_f C_f}{I_z}, \quad e_1 = \frac{1}{M}, \quad e_2 = \frac{l_w}{I_z}.$$

TABLE I
VEHICLE MODEL PARAMETERS

Symbol	Description	Value
M	Total mass of the vehicle	2052 [kg]
l_f	Distance from GC to front axle	1.3 [m]
l_r	Distance from GC to rear axle	1.6 [m]
l_w	Distance from GC to wind impact point	0.4 [m]
l_s	Look-ahead distance	5 [m]
η_t	Tire length contact	0.13 [m]
I_z	Vehicle yaw moment of inertia	2800 [kgm^2]
I_s	Steering system moment of inertia	0.05 [kgm^2]
R_s	Steering gear ratio	16 [-]
B_s	Steering system damping	5.73 [-]
C_f	Front cornering stiffness	57000 [N/rad]
C_r	Rear cornering stiffness	59000 [N/rad]

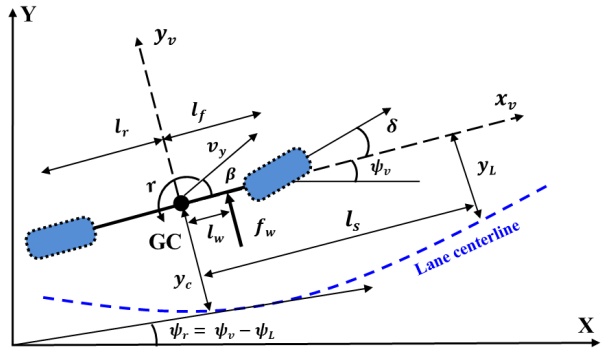

Fig. 1. Lateral vehicle behavior modeling.

B. Driver-in-the-Loop Vehicle Model

For the driving task, the driver is guided on the road by looking at the so-called *near point* and *far point* [20]. These two specific points are respectively characterized by two visual angles θ_{near} and θ_{far}. Note that the driving control process of the driver can be divided into two parts: *compensatory* (represented by $\mathbf{G}_c = K_{d1}\theta_{near}$) and *anticipatory* (represented by $\mathbf{G}_a = K_{d2}\theta_{far}$), which may be executed in parallel [21]. Then, the driver torque can be expressed as

$$T_d = \mathbf{G}_c + \mathbf{G}_a = K_{d_1}\theta_{near} + K_{d_2}\theta_{far} \tag{2}$$

where the gains K_{d_1} and K_{d_2} characterizing the driver's driving style are identified from real-time data. The expressions of two visual angles are given as follows [21]:

$$\begin{aligned} &\theta_{near} = \frac{y_L}{v_x T_p} + \psi_L, \quad \theta_{far} = \theta_1 v_y + \theta_2 r + \theta_3 \delta_d \\ &\theta_1 = \tau_a^2 a_{21}, \quad \theta_2 = \tau_a + \tau_a^2 a_{22}, \quad \theta_3 = \tau_a^2 b_2, \quad \delta_d = \delta R_s \end{aligned} \tag{3}$$

where T_p is the preview time and τ_a represents the anticipatory time of the driver. From (2)-(3), the expression of the driver torque can be rewritten in the form

$$T_d = T_{d_1} v_y + T_{d_2} r + K_{d_1}\psi_L + T_{d_3} y_L + T_{d_4}\delta \tag{4}$$

with $T_{d_1} = K_{d_2}\theta_1\rho$, $T_{d_2} = K_{d_2}\theta_2\rho$, $T_{d_3} = \frac{\rho K_{d_1}}{v_x T_p}$, and $T_{d_4} = \rho K_{d_2}\theta_3 R_s$. From (1) and (4), the diver-in-the-loop vehicle model can be represented as

$$\dot{x}_v = A_v x_v + B T_c + B_w w \tag{5}$$

where

$$A_v = \begin{bmatrix} a_{11} & a_{12} & 0 & 0 & b_1 & 0 \\ a_{21} & a_{22} & 0 & 0 & b_2 & 0 \\ 0 & 1 & 0 & 0 & 0 & 0 \\ 1 & l_s & v_x & 0 & 0 & 0 \\ 0 & 0 & 0 & 0 & 0 & 1 \\ \hat{T}_{s_1} & \hat{T}_{s_2} & K_{d_1}/I_s & T_{d_3} & \hat{T}_{s_3} & T_{s_4} \end{bmatrix}$$

and

$$\hat{T}_{s_1} = T_{s_1} + T_{d_1}, \quad \hat{T}_{s_2} = T_{s_2} + T_{d_2}, \quad \hat{T}_{s_3} = T_{s_3} + T_{d_4}.$$

Based on (5), we propose in the next section a new driver-road-vehicle model to consider *explicitly* the real-time driving activity of the human driver in the control design procedure.

III. Adaptive Authority Allocation for Driver-Automation Shared Control Design

This paper proposes an *adaptive* shared control strategy for LKA systems that can help the human driver in various driving circumstances. In [9], the driver's need for assistance according to his/her driving workload and performance has been investigated. This study points out that the level of assistance should be designed to relieve the driver in overload and underload conditions, see Fig. 2. Moreover, to manage effectively the driver-automation conflict, the driver should always remain in the control loop and she/he should receive a *continuous* feedback from the automation [7]. The proposed shared control strategy follows these guidelines to deal with the human-machine interaction involved in the design procedure. To this end, the assistance torque T_c is modulated in accordance with the real-time driving activity of the driver

$$T_c = \mu(\theta_d)u \tag{6}$$

where the fictive torque u will be designed and the normalized variable θ_d represents the driver's real-time driving activity as discussed later. Remark that the weighting function $\mu(\theta_d)$ in (6) allows for a *continuous* assistance from the LKA system. Inspired by the generalized Bell-shape function, the weighting function $\mu(\theta_d)$ takes the following form:

$$\mu(\theta_d) = \frac{1}{1 + \left|\frac{\theta_d - \omega_3}{\omega_1}\right|^{2\omega_2}} + \mu_{\min} \tag{7}$$

where $\omega_1 = 0.355$, $\omega_2 = -2$, $\omega_3 = 0.5$ and $\mu_{\min} = 0.1$.

Remark 1. The parameters of $\mu(\theta_d)$ in (7) are parameterized such that this can represent the U-shape function characterizing the driver's need for assistance, see Figs. 2 and 3. Observe from (6) that the maximal level of assistance $\mu_{\max} = 1$ corresponds to the case where $u = T_c$. A deadband of minimal level of assistance is necessary to avoid the driver-automation conflict in cases where the driver is not purposely counter steering, see Fig. 3. This deadband should be sufficiently large, which is ensured here by the generalized Bell shape, to allow for a maximum driver reaction torque in shared control mode [2]. The value $\mu_{\min} = 0.1$ is chosen such that T_c can benefit from a large variation range of $\mu(\theta_d)$, i.e. the real-time information on the driver's driving activity can be effectively

exploited by the shared controller. However, an unnecessarily small value of $\mu_{\min}$ could induce the design conservatism.

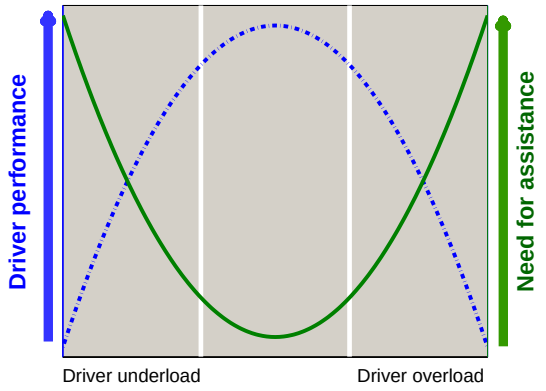

Fig. 2. U-shape function representing the driver's need for assistance according to her/his driving workload and performance [9].

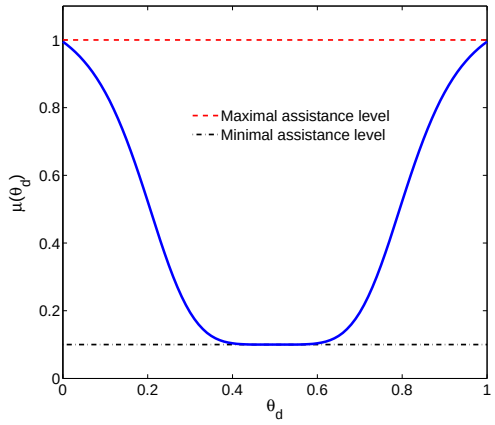

Fig. 3. Weighting factor $\mu(\theta_d)$ as a function of the driver's real-time driving activity with $\omega_1 = 0.355$, $\omega_2 = -2$, $\omega_3 = 0.5$ and $\mu_{\min} = 0.1$.

By taking into account the driving variable θ_d into (4), the driver-in-the-loop vehicle model used for the control design can be then deduced from (5)-(6) as follows:

$$\boldsymbol{\Sigma}_v\left(v_x, \mu(\theta_d)\right): \ \dot{x}_v = A_v x_v + B_u u + B_w w \tag{8}$$

where

$$A_v = \begin{bmatrix} a_{11} & a_{12} & 0 & 0 & b_1 & 0 \\ a_{21} & a_{22} & 0 & 0 & b_2 & 0 \\ 0 & 1 & 0 & 0 & 0 & 0 \\ 1 & l_s & v_x & 0 & 0 & 0 \\ 0 & 0 & 0 & 0 & 0 & 1 \\ \tilde{T}_{d1} & \tilde{T}_{d2} & \tilde{K}_{d1} & \tilde{T}_{d3} & \tilde{T}_{d4} & T_{s4} \end{bmatrix}, \ B_u = \begin{bmatrix} 0 \\ 0 \\ 0 \\ 0 \\ 0 \\ \tilde{\rho} \end{bmatrix}.$$

For system (8), the real-time driving activity of the driver is also taken into account in the driver model (4) as follows:

$$\tilde{T}_{d_1} = T_{s1} + (1-\mu(\theta_d))\,T_{d_1}, \ \tilde{T}_{d_2} = T_{s2} + (1-\mu(\theta_d))\,T_{d_2},$$
$$\tilde{T}_{d_3} = (1-\mu(\theta_d))\,T_{d_3}, \ \ \tilde{T}_{d_4} = T_{s3} + (1-\mu(\theta_d))\,T_{d_4},$$
$$\tilde{K}_{d_1} = (1-\mu(\theta_d))\,K_{d_1}/I_s, \ \ \tilde{\rho} = \mu(\theta_d)\rho.$$

For the proposed method, the driver activity variable θ_d depends on two factors: (i) the measured driver torque T_d, and (ii) the driver state variable ($0 \leq DS \leq 1$) provided by the driver monitoring system [5], [22]:

$$\theta_d = 1 - e^{-(\sigma_1 T_{dN})^{\sigma_2} DS^{\sigma_3}} \tag{9}$$

where the tuning parameters are given by $\sigma_1 = 2$ and $\sigma_2 = \sigma_3 = 3$. The normalized driver torque is defined as $T_{dN} = \left|\frac{T_d}{T_{d\max}}\right|$ where $T_{d\max}$ is the maximal torque can be delivered by the driver. The parameter σ_1 is used together with T_{dN} to represent the involvement level of the driver in the driving tasks whereas the parameters σ_2 and σ_3 represent the degree of influence of the driver torque and the driver state on the driver activity variable θ_d. These three parameters are tuned such that the information from the supervision level (T_d and DS) are judiciously exploited in (9) to represent the real-time driving activity of the driver. Fig. 4 shows that when the driver torque and/or the driver state remain(s) small (which means that the driver activity is not significant), the corresponding values of the normalized variable θ_d are small and a high level of assistance is required. When the driver is highly involved in his/her driving tasks, i.e. θ_d tends to 1 (for example in the case where the driver needs to realize a difficult driving task), an important level of assistance from the LKA system is also required to help him/her. With a constant driver torque (respectively driver state), the driving activity of the driver increases according to the value of the driver state DS (respectively driver torque).

For the driver-road-vehicle system (8), six physical sensors are necessary to measure all vehicle states for a full state-feedback control scheme. However, since the measurements of the lateral velocity v_y and the steering angle rate $\dot{\delta}$ are *unavailable*, such a control scheme cannot be applied here. In addition, the dynamics of system (8) depends strongly on the vehicle speed v_x and the driver activity variable θ_d which are *time-varying*. In next section, we develop a *sensor reduction* method based on T-S fuzzy output feedback control and LMI formulation to overcome these practical issues.

IV. Sensor Reduction via Fuzzy Dynamic Output Feedback Control

Sensor reduction based control approach can be formulated as an output feedback control problem [23]. To reduce the number of feedback sensors, we first derive the conditions to design a fuzzy output feedback controller using Lyapunov stability arguments and LMI techniques. Then, the application of theoretical results to the shared lateral control is presented.

A. Closed-Loop Description of Takagi-Sugeno Fuzzy Systems

Consider the following T-S fuzzy model [11]:

$$\begin{aligned} \dot{x} &= \sum_{i=1}^{r} \eta_i(\theta)\left(A_i x + B_i^u u + B_i^w w\right) \\ z &= \sum_{i=1}^{r} \eta_i(\theta)\left(C_i^z x + D_i^{zu} u + D_i^{zw} w\right) \\ y &= \sum_{i=1}^{r} \eta_i(\theta)\left(C_i^y x + D_i^{yw} w\right) \end{aligned} \tag{10}$$

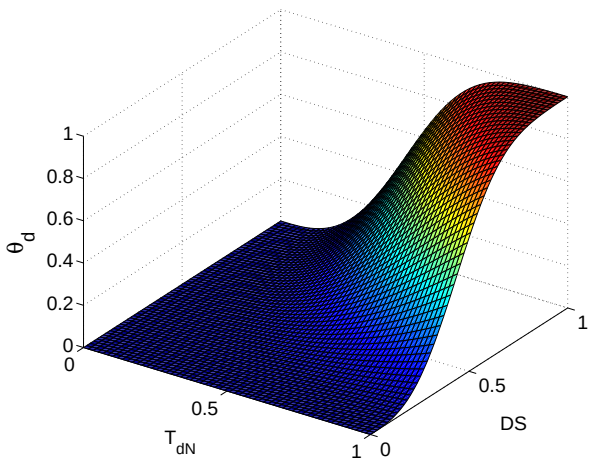

Fig. 4. Driver activity function with $\sigma_1 = 2$, $\sigma_2 = \sigma_3 = 3$.

where $x \in \mathbb{R}^{n_x}$ is the system state, $u \in \mathbb{R}^{n_u}$ is the control input, $w \in \mathbb{R}^{n_w}$ is the system disturbance, $y \in \mathbb{R}^{n_y}$ is the measured output, $z \in \mathbb{R}^{n_z}$ is the performance output, and $\theta \in \mathbb{R}^k$ is the vector of measured premise variables. The matrices of appropriate dimensions A_i, B_i^u, B_i^w, C_i^z, D_i^{zu}, D_i^{zw}, C_i^y and D_i^{yw}, $i \in \{1, \dots, r\}$, represent the set of r local linear subsystems. The scalar membership functions $\eta_i(\theta)$ satisfy the following convex sum property:

$$\sum_{i=1}^{r} \eta_i(\theta) = 1, \quad \eta_i(\theta) \geq 0, \quad i \in \{1, \dots, r\}.$$

The fuzzy output feedback controller is constructed based on the following dynamic parallel distributed compensation law:

$$\begin{aligned} \dot{x}_c &= \sum_{i=1}^{r} \sum_{j=1}^{r} \eta_i(\theta)\eta_j(\theta) A_{ij}^c x_c + \sum_{i=1}^{r} \eta_i(\theta) B_i^c y \\ u_c &= \sum_{i=1}^{r} \eta_i(\theta) C_i^c x_c + D^c y, \quad x_c(0) = 0 \end{aligned} \tag{11}$$

where $x_c \in \mathbb{R}^{n_x}$, $u_c \in \mathbb{R}^{n_u}$ are respectively the state and the output of the controller. Let us define $x_{cl}^\top = \begin{bmatrix} x^\top & x_c^\top \end{bmatrix}$, from (10) and (11) the closed-loop system is given as follows:

$$\begin{aligned} \dot{x}_{cl} &= \sum_{i=1}^{r} \sum_{j=1}^{r} \eta_i(\theta)\eta_j(\theta) \left(\mathbb{A}_{ij} x_{cl} + \mathbb{B}_{ij}^w w \right) \\ z &= \sum_{i=1}^{r} \sum_{j=1}^{r} \eta_i(\theta)\eta_j(\theta) \left(\mathbb{C}_{ij} x_{cl} + \mathbb{D}_{ij}^w w \right) \end{aligned} \tag{12}$$

where

$$\begin{aligned} \mathbb{A}_{ij} &= \begin{bmatrix} A_i + B_i^u D^c C_j^y & B_i^u C_j^c \\ B_i^c C_j^y & A_{ij}^c \end{bmatrix}, \\ \mathbb{B}_w^{ij} &= \begin{bmatrix} B_i^w + B_i^u D^c D_j^{yw} \\ B_i^c D_j^{yw} \end{bmatrix}, \\ \mathbb{C}_{ij} &= \begin{bmatrix} C_i^z + D_i^{zu} D^c C_j^y & D_i^{zu} C_j^c \end{bmatrix}, \\ \mathbb{D}_w^{ij} &= D_i^{zw} + D_i^{zu} D^c D_j^{yw}. \end{aligned}$$

The output of the fuzzy controller (11) is given by

$$u_c = \sum_{i=1}^{r} \eta_i(\theta) \left(\mathbb{K}_i x_{cl} + K_i^w w \right)$$

where $\mathbb{K}_i = \begin{bmatrix} D^c C_i^y & C_i^c \end{bmatrix}$ and $K_i^w = D^c D_i^{yw}$.

Notation. The following notations are introduced for brevity. For a matrix X, $X^\top$ denotes its transpose. For any square matrix X, $X > 0$ means X is symmetric positive definite and $\mathrm{He}(X) = X + X^\top$. I denotes the identity matrix of appropriate dimension. $(\star)$ stands for matrix blocks that can be deduced by symmetry. $\mathrm{diag}(\cdot)$ denotes a block diagonal matrix formed by the blocks given in the parenthesis. For brevity, the scalar function $\eta_i(\theta)$ is denoted by η_i, $i \in \{1, \dots, r\}$.

B. Fuzzy Model-Based Output Feedback Control Design

For real-world applications, it is important to consider not only the stability but also other performance specifications. Hereafter, a constructive LMI-based design for stability, decay rate and $\mathcal{H}_\infty$ performance of the closed-loop system (12) is derived.

Definition 1. The T-S system (12) is stable with a decay rate $\alpha > 0$ if there exists a positive definite function

$$\mathbb{V}(x_{cl}) = x_{cl}^\top \mathbb{P} x_{cl}, \quad \mathbb{P} > 0 \tag{13}$$

such that

$$\dot{\mathbb{V}}(x_{cl}) < -2\alpha \mathbb{V}(x_{cl}) \tag{14}$$

for any solution x_{cl} of (12). The speed of response of the closed-loop system is related to the decay rate [11].

Definition 2. If the T-S system (12) is stable and satisfies

$$\int_0^\infty z(t)^\top z(t) dt < \gamma^2 \int_0^\infty w(t)^\top w(t) dt \tag{15}$$

for $x_{cl}(0) = 0$. Then, the $\mathcal{H}_\infty$ norm of (12) is said to be less than γ. The constraint (15) can be interpreted as a disturbance rejection performance. This constraint is also useful to enforce robust stability [24].

The following theorem allows for the design of a dynamic output feedback controller (11) satisfying the closed-loop properties defined in (14) and (15).

Theorem 1. Given a T-S fuzzy system (10) and a positive scalar α. Assume there exist positive definite matrices $\mathbf{P_{11}} \in \mathbb{R}^{n_x \times n_x}$, $\mathbf{X_{11}} \in \mathbb{R}^{n_x \times n_x}$, matrices $\hat{\mathbf{A}}_{ij} \in \mathbb{R}^{n_x \times n_x}$, $\hat{\mathbf{B}}_i \in \mathbb{R}^{n_x \times n_y}$, $\hat{\mathbf{C}}_i \in \mathbb{R}^{n_u \times n_x}$ and $\hat{\mathbf{D}} \in \mathbb{R}^{n_u \times n_y}$ for $i, j \in \{1, \dots, r\}$, and a positive scalar $\gamma > 0$ such that

$$\begin{bmatrix} \mathbf{X_{11}} & I \\ I & \mathbf{P_{11}} \end{bmatrix} > 0 \tag{16}$$

$$\sum_{i=1}^{r} \sum_{j=1}^{r} \eta_i \eta_j \Xi_{ij} < 0 \tag{17}$$

where the quantity Ξ_{ij} is defined as

$$\Xi_{ij} = \begin{bmatrix} \Xi_{ij}^{[11]} & \Xi_{ij}^{[12]} & \Xi_{ij}^{[13]} & \Xi_{ij}^{[14]} \\ \star & \Xi_{ij}^{[22]} & \Xi_{ij}^{[23]} & \Xi_{ij}^{[24]} \\ \star & \star & -\gamma I & \Xi_{ij}^{[34]} \\ \star & \star & \star & -\gamma I \end{bmatrix} \tag{18}$$

and $\Xi_{ij}^{[11]} = \mathrm{He}(A_i \mathbf{X_{11}} + B_i^u \hat{\mathbf{C}}_j + \alpha \mathbf{X_{11}})$, $\Xi_{ij}^{[12]} = A_i + B_i^u \hat{\mathbf{D}} C_j^y + \hat{\mathbf{A}}_{ij}^\top + 2\alpha I$, $\Xi_{ij}^{[13]} = B_i^u \hat{\mathbf{D}} D_j^{yw} + B_i^w$, $\Xi_{ij}^{[22]} =$

$\mathrm{He}(\mathbf{P_{11}}A_i + \hat{\mathbf{B}}_i C_j^y + \alpha \mathbf{P_{11}})$, $\Xi_{ij}^{[23]} = \mathbf{P_{11}}B_i^w + \hat{\mathbf{B}}_i D_j^{yw}$, $\Xi_{ij14} = (C_i^z \mathbf{X_{11}} + D_i^{zu}\hat{\mathbf{C}}_j)^\top$, $\Xi_{ij}^{[24]} = (C_i^z + D_i^{zu}\hat{\mathbf{D}}C_j^y)^\top$, $\Xi_{ij}^{[34]} = (D_i^{zw} + D_i^{zu}\hat{\mathbf{D}}D_j^{yw})^\top$.

Let P_{12} and X_{12} be two *nonsingular* matrices such that

$$\mathbf{P_{11}}\mathbf{X_{11}} + P_{12}X_{12}^\top = I. \tag{19}$$

Then, the fuzzy output feedback controller (11) with the feedback gains defined by

$$\begin{aligned}
D^c &= \hat{\mathbf{D}} \\
C_i^c &= \left(\hat{\mathbf{C}}_i - D^c C_i^y \mathbf{X_{11}}\right) X_{12}^{-\top} \\
B_i^c &= P_{12}^{-1}\left(\hat{\mathbf{B}}_i - \mathbf{P_{11}}B_i^u D^c\right) \\
A_{ij}^c &= P_{12}^{-1}\begin{pmatrix} \hat{\mathbf{A}}_{ij} - \mathbf{P_{11}}\left(A_i + B_i^u D^c C_j^y\right)\mathbf{X_{11}} \\ - P_{12}B_i^c C_j^y \mathbf{X_{11}} - \mathbf{P_{11}}B_i^u C_j^c X_{12}^\top \end{pmatrix} X_{12}^{-\top}
\end{aligned} \tag{20}$$

for $i, j \in \{1, \ldots, r\}$, solves the control problem stated above.

Proof. Conditions (16) and (19) imply the existence of two matrices P_{22} and X_{22} such that the following block matrices:

$$\mathbb{P} = \begin{bmatrix} \mathbf{P_{11}} & P_{12} \\ P_{12}^\top & P_{22} \end{bmatrix}, \quad \mathbb{X} = \mathbb{P}^{-1} = \begin{bmatrix} \mathbf{X_{11}} & X_{12} \\ X_{12}^\top & X_{22} \end{bmatrix}$$

are positive definite [24]. Note that the same properties guarantee the existence of two nonsingular matrices P_{12} and X_{12}. The T-S fuzzy system (12) is stable while satisfying the decay rate (14) and the $\mathcal{H}_\infty$ performance (15) if

$$\dot{\mathbb{V}}(x_{cl}) + \frac{1}{\gamma} z^\top z - \gamma w^\top w < -2\alpha \mathbb{V}(x_{cl}) \tag{21}$$

Using the *explicit* expressions of the closed-loop system (12) and the Lyapunov function (13), (21) can be rewritten as

$$\xi^\top \Gamma \xi < 0 \tag{22}$$

where $\xi^\top = \begin{bmatrix} x_{cl}^\top & w^\top \end{bmatrix}$ and

$$\Gamma = \sum_{i=1}^{r}\sum_{j=1}^{r} \eta_i \eta_j \left\{ \begin{bmatrix} \mathrm{He}\left(\mathbb{P}\mathbb{A}_{ij} + \alpha \mathbb{P}\right) & \star \\ \mathbb{P}\mathbb{B}_{ij}^{w\top} & -\gamma I \end{bmatrix} + \frac{1}{\gamma}\Lambda_{ij}^\top \Lambda_{ij} \right\}$$

with $\Lambda_{ij} = \begin{bmatrix} \mathbb{C}_{ij} & \mathbb{D}_{ij}^w \end{bmatrix}$. It is clear that (22) is verified if $\Gamma < 0$. By Schur complement lemma [15], this latter is equivalent to

$$\sum_{i=1}^{r}\sum_{j=1}^{r} \eta_i \eta_j \begin{bmatrix} \mathrm{He}(\mathbb{P}\mathbb{A}_{ij} + \alpha\mathbb{P}) & \star & \star \\ \mathbb{B}_{ij}^{w\top}\mathbb{P} & -\gamma I & \star \\ \mathbb{C}_{ij} & \mathbb{D}_{ij}^w & -\gamma I \end{bmatrix} < 0 \tag{23}$$

Let us define $\Pi = \begin{bmatrix} \mathbf{X_{11}} & I \\ X_{12}^\top & 0 \end{bmatrix}$. Pre- and postmultiplying (23) with $\mathrm{diag}\left(\Pi^\top, I, I\right)$ and its transpose leads to

$$\sum_{i=1}^{r}\sum_{j=1}^{r} \eta_i \eta_j \begin{bmatrix} \Pi^\top \Phi_{ij} \Pi & \star & \star \\ \mathbb{B}_{ij}^{w\top}\mathbb{P}\Pi & -\gamma I & \star \\ \mathbb{C}_{ij}\Pi & \mathbb{D}_{ij}^w & -\gamma I \end{bmatrix} < 0 \tag{24}$$

where $\Phi_{ij} = \mathbb{A}_{ij}^\top \mathbb{P} + \mathbb{P}\mathbb{A}_{ij} + \alpha\mathbb{P}$. The convexification procedure of (24) can be performed with the following definitions:

$$\begin{aligned}
\hat{\mathbf{A}}_{ij} &= P_{12}A_{ij}^c X_{12}^\top + \mathbf{P_{11}}\left(A_i + B_i^u D^c C_j^y\right)\mathbf{X_{11}} \\
&\quad + P_{12}B_i^c C_j^y \mathbf{X_{11}} + \mathbf{P_{11}}B_i^u C_j^c X_{12}^\top \\
\hat{\mathbf{B}}_i &= P_{12}B_i^c + \mathbf{P_{11}}B_i^u D^c \\
\hat{\mathbf{C}}_i &= C_i^c X_{12}^\top + D^c C_i^y \mathbf{X_{11}} \\
\hat{\mathbf{D}} &= D^c
\end{aligned} \tag{25}$$

for $i, j \in \{1, \ldots, r\}$. Using (25), the following identities can be straightforwardly obtained:

$$\Pi^\top \mathbb{P}\mathbb{A}_{ij}\Pi = \begin{bmatrix} A_i\mathbf{X_{11}} + B_i^u\hat{\mathbf{C}}_j & A_i + B_i^u\hat{\mathbf{D}}C_j^y \\ \hat{\mathbf{A}}_{ij} & \mathbf{P_{11}}A_i + \hat{\mathbf{B}}_i C_j^y \end{bmatrix},$$

$$\mathbb{C}_{ij}\Pi = \begin{bmatrix} C_i^z\mathbf{X_{11}} + D_i^{zu}\hat{\mathbf{C}}_j & C_i^z + D_i^{zu}\hat{\mathbf{D}}C_j^y \end{bmatrix},$$

$$\Pi^\top \mathbb{P}\mathbb{B}_{ij}^w = \begin{bmatrix} B_i^u\hat{\mathbf{D}}D_j^{yw} + B_i^w \\ \mathbf{P_{11}}B_i^w + \hat{\mathbf{B}}_i D_j^{yw} \end{bmatrix}, \quad \Pi^\top\mathbb{P}\Pi = \begin{bmatrix} \mathbf{X_{11}} & I \\ I & \mathbf{P_{11}} \end{bmatrix}.$$

Replacing the explicit expressions of $\Pi^\top\mathbb{P}\mathbb{A}_{ij}\Pi$, $\Pi^\top\mathbb{P}\mathbb{B}_{ij}^w$ and $\mathbb{C}_{ij}\Pi$ into (24) leads directly to (17). Moreover, the feedback gains (20) can be easily recovered from the change of variable (25). Thus, the proof of Theorem 1 can be concluded. □

Remark 2. Condition (17) is represented in the form of a parameterized linear matrix inequality. Here, the relaxation result in [25] is applied to convert (17) into the following finite set of LMIs:

$$\begin{aligned}
&\Xi_{ii} < 0, \quad i \in \{1, \ldots, r\} \\
&\frac{2}{r-1}\Xi_{ii} + \Xi_{ij} + \Xi_{ji} < 0, \quad i, j \in \{1, \ldots, r\},\ i < j
\end{aligned} \tag{26}$$

Remark 3. The equation (19) admits *infinite* solutions of P_{12} and X_{12} parameterizing an *infinite* number of controllers (11). However, these controllers induce the same decay rate and $\mathcal{H}_\infty$ performance since P_{12} and X_{12} are not *explicitly* involved in the LMIs of Theorem 1. Therefore, the choice of P_{12} and X_{12} satisfying (19) is *irrelevant* for the proposed control method. One possible way to determine these nonsingular matrices is based on the well-known singular value decomposition in conjunction with the Cholesky factorization, namely

$$P_{12}X_{12}^\top = I - \mathbf{P_{11}}\mathbf{X_{11}} = U\Sigma V^\top = UR^\top R V^\top. \tag{27}$$

Then, one has clearly that $P_{12} = UR^\top$ and $X_{12} = VR^\top$.

The following theorem summarizes the discussions given in Remarks 2, 3 and provides LMI-based design conditions for the considered control problem.

Theorem 2. Given a T-S fuzzy system (10) and a positive scalar α. If there exist positive definite matrices $\mathbf{P_{11}} \in \mathbb{R}^{n_x \times n_x}$, $\mathbf{X_{11}} \in \mathbb{R}^{n_x \times n_x}$, matrices $\hat{\mathbf{A}}_{ij} \in \mathbb{R}^{n_x \times n_x}$, $\hat{\mathbf{B}}_i \in \mathbb{R}^{n_x \times n_y}$, $\hat{\mathbf{C}}_i \in \mathbb{R}^{n_u \times n_x}$ and $\hat{\mathbf{D}} \in \mathbb{R}^{n_u \times n_y}$ for $i, j \in \{1, \ldots, r\}$ and a positive scalar γ such that the LMIs (16) and (26) are verified where the quantity Ξ_{ij} is defined in (18). Then, the T-S fuzzy system (10) is stabilized by the output feedback controller (11) with an $\mathcal{H}_\infty$ norm less than γ. The controller gains are given in (20) where two nonsingular matrices P_{12} and X_{12} can be computed from (27).

Remark 4. Theorem 2 provides a systematic method to design a fuzzy output feedback controller (11). The design procedure is formulated as a convex optimization so that the feedback gains in (20) can be effectively computed with available numerical toolboxes, e.g. YALMIP toolbox [26].

In what follows, the application of Theorem 2 to the shared control design of the studied LKA system is highlighted.

C. Design of Shared Controller for LKA Systems

Since the lateral speed v_y and the steering rate $\dot{\delta}$ are assumed to be *unmeasurable*, the output equation of the T-S fuzzy model (10) for the driver-vehicle system is given by

$$y = \sum_{i=1}^{r} \eta_i(\theta)(C_i^y x + D_i^{yw} w)$$

where

$$C_i^y = C = \begin{bmatrix} 0 & 1 & 0 & 0 & 0 & 0 \\ 0 & 0 & 1 & 0 & 0 & 0 \\ 0 & 0 & 0 & 1 & 0 & 0 \\ 0 & 0 & 0 & 0 & 1 & 0 \end{bmatrix}, \quad D_i^{yw} = 0.$$

To take into account the $\mathcal{H}_\infty$ performance (15), the controlled output is defined as follows:

$$\begin{aligned} z &= \mathcal{W} \begin{bmatrix} a_y & \dot{\psi}_r & \theta_{near} & \theta_{far} & \dot{\delta} \end{bmatrix}^\top \\ \mathcal{W} &= \text{diag}(q_{a_y},\ q_{\dot{\psi}_r},\ q_{\theta_{near}},\ q_{\theta_{far}},\ q_{\dot{\delta}}) \end{aligned} \tag{28}$$

where q_{a_y}, $q_{\dot{\psi}_r}$, $q_{\theta_{near}}$, $q_{\theta_{far}}$ and $q_{\dot{\delta}}$ are the weighting coefficients. Note that the lane keeping performance is represented by the *near* and *far* visual angles in (28) which allow respectively for the consideration of the driver's *compensatory* and *anticipatory* behaviors, see (3). The driver's comfort is represented by the lateral acceleration a_y and the relative yaw rate $\dot{\psi}_r$ as

$$a_y = v_x r, \quad \dot{\psi}_r = r - v_x \rho_r.$$

The steering wheel rate $\dot{\delta}$ is introduced in (28) to guarantee a desired comfort for the steering correction. Then, the performance output matrices in (10) of (8) are given by

$$\begin{aligned} C_i^z &= \mathcal{W} \begin{bmatrix} 0 & v_x & 0 & 0 & 0 & 0 \\ 0 & 1 & 0 & 0 & 0 & 0 \\ 0 & 0 & 1 & \frac{1}{v_x T_p} & 0 & 0 \\ \theta_1 & \theta_2 & 0 & 0 & \theta_3 & 0 \\ 0 & 0 & 0 & 0 & 0 & 1 \end{bmatrix}, \quad D_i^{zu} = 0 \\ D_i^{zw} &= \begin{bmatrix} 0 & 0 & 0 & 0 & 0 \\ 0 & -v_x & 0 & 0 & 0 \end{bmatrix}^\top, \quad i \in \{1, \ldots, r\} \end{aligned} \tag{29}$$

Note that the system matrices in (8) and (29) depend *nonlinearly* on the vehicle speed (i.e. v_x and $1/v_x$), and the driver variable $\mu(\theta_d)$ which are measured and bounded

$$v_{\min} \le v_x \le v_{\max}, \quad \mu_{\min} \le \mu(\theta_d) \le \mu_{\max},$$

where $v_{\min} = 9$, $v_{\max} = 30$, $\mu_{\min} = 0.1$ and $\mu_{\max} = 1$. The T-S fuzzy modeling of the driver-in-the-loop vehicle system could be done with the natural choice of premise variables $\theta_\star = \begin{bmatrix} v_x & 1/v_x & \mu(\theta_d) \end{bmatrix}^\top \in \mathbb{R}^3$. Using the sector nonlinearity approach [11], this choice leads to an exact T-S fuzzy representation (10) with $r_\star = 2^3 = 8$ linear subsystems. However, this T-S fuzzy driver-vehicle model would be too *costly* in terms of numerical computation for control purposes, and especially for real-time implementation. Here, the strong relationship between v_x and $1/v_x$ is exploited through the first order Taylor's approximation to reduce significantly the numerical complexity of the proposed control method

$$\frac{1}{v_x} = \frac{1}{v_0} + \frac{1}{v_1}\Delta_x, \quad v_x \cong v_0 \left(1 - \frac{v_0}{v_1}\Delta_x\right) \tag{30}$$

where $\Delta_{\min} \le \Delta_x \le \Delta_{\max}$, $\Delta_{\min} = -1$ and $\Delta_{\max} = 1$. The new measured time-varying parameter Δ_x is used to describe the variation of v_x between its lower and upper bounds. The two constants v_0 and v_1 are given by

$$v_0 = \frac{2v_{\min}v_{\max}}{v_{\min} + v_{\max}}, \quad v_1 = \frac{2v_{\min}v_{\max}}{v_{\min} - v_{\max}}.$$

Replacing (30) into (8), the premise variables can be now defined as $\theta = \begin{bmatrix} \Delta_x & \mu(\theta_d) \end{bmatrix}^\top \in \mathbb{R}^2$. By the sector nonlinearity approach, the corresponding T-S fuzzy driver-vehicle model has only $r = 2^2 = 4$ linear subsystems

$$\begin{aligned} &\boldsymbol{\Sigma}_{v1}(\Delta_{\min}, \mu_{\min}), \quad \boldsymbol{\Sigma}_{v2}(\Delta_{\min}, \mu_{\max}), \\ &\boldsymbol{\Sigma}_{v3}(\Delta_{\max}, \mu_{\min}), \quad \boldsymbol{\Sigma}_{v4}(\Delta_{\max}, \mu_{\max}). \end{aligned}$$

The corresponding membership functions are defined as

$$\begin{aligned} \eta_1 &= \Omega_{\Delta 1}\Omega_{\mu 1}, \quad \eta_2 = \Omega_{\Delta 1}\Omega_{\mu 2}, \\ \eta_3 &= \Omega_{\Delta 2}\Omega_{\mu 1}, \quad \eta_4 = \Omega_{\Delta 2}\Omega_{\mu 2}, \end{aligned}$$

where

$$\begin{aligned} \Omega_{\Delta 1} &= \frac{\Delta_{\max} - \Delta_x}{\Delta_{\max} - \Delta_{\min}}, \quad \Omega_{\Delta 2} = \frac{\Delta_x - \Delta_{\min}}{\Delta_{\max} - \Delta_{\min}}, \\ \Omega_{\mu 1} &= \frac{\mu_{\max} - \mu(\theta_d)}{\mu_{\max} - \mu_{\min}}, \quad \Omega_{\mu 2} = \frac{\mu(\theta_d) - \mu_{\min}}{\mu_{\max} - \mu_{\min}}. \end{aligned}$$

Theorem 2 can be now applied to the T-S fuzzy driver-in-the-loop vehicle model to design the output feedback controller (11) for shared control purposes.

V. Simulation and Hardware Experiments

This section presents the results of a series of both simulation and hardware experiments to demonstrate the practical performance of the proposed shared control method.

A. Numerical Simulation

All simulations are conducted using Matlab/Simulink platform with the nonlinear vehicle model given in [10]. The sensorimotor driver model proposed in [27] is used to simulate the behaviors of a human driver. The test track is depicted in Fig. 5 (left), which consists of a straight road section followed by four curves with different radius $R_1 = 50$ [m], $R_2 = 33$ [m], $R_3 = 25$ [m] and $R_4 = 20$ [m]. Fig. 5 (right) shows the road curvature and the vehicle speed corresponding to the considered test track.

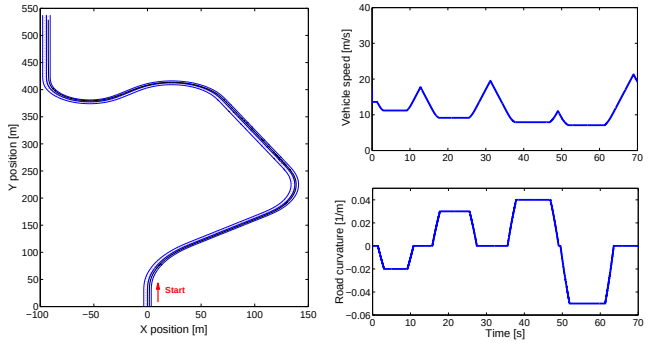

Fig. 5. Vehicle trajectory (left), vehicle speed and road curvature (right).

1) Scenario 1 [Lane Keeping Control Performance]: This test is composed of three phases. For the first phase (from $t = 0s$ to $t = 15s$), the vehicle is *fully* controlled by the designed shared steering controller ($T_d = 0$), see Fig. 6 (a). Observe in Fig. 6 (b) that $\mu(\theta_d) = 1$ during this period which means that the maximal level of assistance is required to perform the driving task. In the second phase (from $t = 15s$ to $t = 50s$), both the driver and the shared controller are involved in the driving process. During this maneuver, the weighting parameter $\mu(\theta_d)$ decreases progressively to 0.4 (respectively 0.2) for the second (respectively third) curve taking. This means that only a small level of assistance is required to assist the driver in these situations. The third phase begins at the end of the third curve where the driver torque T_d decreases quickly to zero and the parameter $\mu(\theta_d)$ tends to 1. This means that the shared controller has a full control authority during this phase as indicated in Fig. 6 (from $t = 50s$ to $t = 70s$).

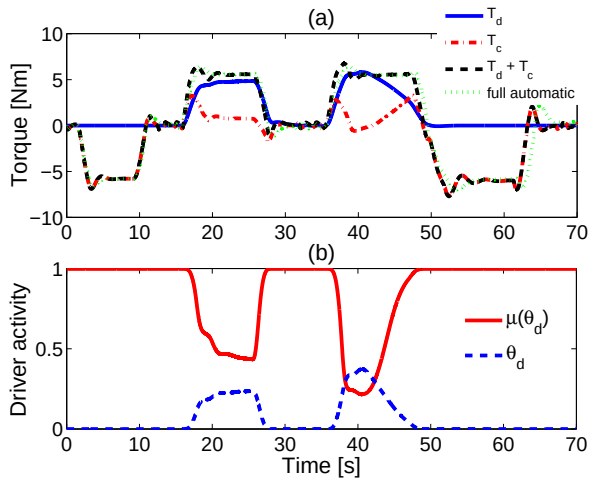

Fig. 6. Lane keeping maneuver: (a) steering torques in shared control, (b) control authority allocation in accordance with the driver's real-time activity.

Fig. 6 (a) shows also the comparison of the total torque (black dashed line) given by the driver model T_d (blue solid line) and the shared controller T_c (red dashdot line), and that provided by a designed *full automatic controller*. The latter torque is computed by fixing $\mu(\theta_d) = 1$ and the driver model is not taken into account in the control design procedure. It is clearly observed that the steering action of the shared controller is *adaptively* computed in accordance with the driver's real-time activity. Note that the total torque is close to that provided by the *full automatic controller* (green dotted line). However, the responses of the shared controller are slightly faster thank to the consideration of θ_{far} (i.e. the driver's anticipatory behavior) in the control design. This allows for an improvement of the control performance in terms of driver's comfort.

2) Scenario 2 [Human-in-the-Loop Control Performance]: This test aims to show the interest of considering the driver model (2) into the control design. To this end, we examine the control performance in two following *shared control* cases.

- Case 1: the shared controller is used together with the driver model to perform the lane keeping task for the driving test track shown in Fig. 5.
- Case 2: the full automatic controller is used with the driver model for the same driving task.

The comparison of the *near* visual angle θ_{near} obtained with two above cases is presented in Fig. 7 (a). Observe that small values of θ_{near} are achieved with Case 1 where its maximal value does not exceed $\pm 10°$. In addition, the shared controller allows the driver model to perform better the taking of curves without overshoot of θ_{far}, see Fig. 7 (b). The overshoot of θ_{far} means that the vehicle has an under-steering behavior. Fig. 7 (c) shows the comparison of the lateral deviation errors, remark that this error in Case 1 has an opposite sign compared to the road curvature, which means that the vehicle slightly cuts the bends to minimize θ_{far}. This result points out the interest of considering the driver's behaviors in the control design of the shared lane keeping driving process.

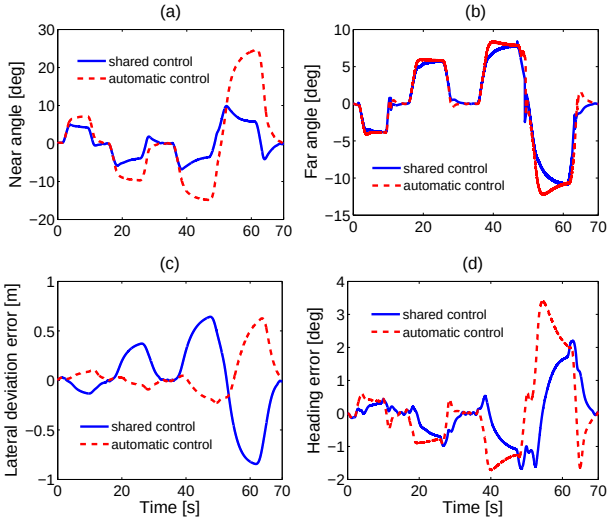

Fig. 7. Control performance comparison between shared controller and full automatic controller.

B. Experimental Validation

1) SHERPA Interactive Dynamic Driving Simulator: This advanced simulator is in the form of a Peugeot 206 vehicle fixed on a Stewart platform, the whole is positioned in front of five flat panel displays providing a visual field of $240°$, see Fig. 8. Based on a distributed computing architecture, this complex simulator is structured around a SCANeR network connecting fifteen PC-type workstations. The whole software of the SHERPA simulator is developed with RTMaps environment composed by several modules which are in charge of different tasks: perception, planning, driver monitoring, human-machine interface. This driving simulator is equipped with a Continental driver monitoring system which indicates the information on the driver's drowsiness/distraction and provides the driver state variable DS used in (9). In what follows, all experiments have been carried out with the SHERPA simulator and a human driver.

Note that for the control design, the driver-road-vehicle model (8) has been first identified and then *experimentally* validated with the data collected from the SHERPA simulator, see also [5], [10]. For illustrations, Fig. 9 shows the validation

Fig. 8. SHERPA driving simulator (left); steering torque sensor and Continental driver monitoring system (right).

results obtained with the database of a test track, located in Satory, 20 km west of Paris, France. We can see that this real-world track consists of several curved sections including tight bends, and the vehicle speed corresponding to the validation test is strongly time-varying as indicated in Figs. 9 (a) and (b). Observe that the responses of (8) are highly close to the behaviors of the SHERPA simulator even when the driver *purposely* performs a zigzag driving pattern on a straight road section to produce high-frequency control inputs, see Figs. 9 (c), (d), (e) and (f). Therefore, the driver-road-vehicle model (8) can be exploited for the design of shared lateral controllers.

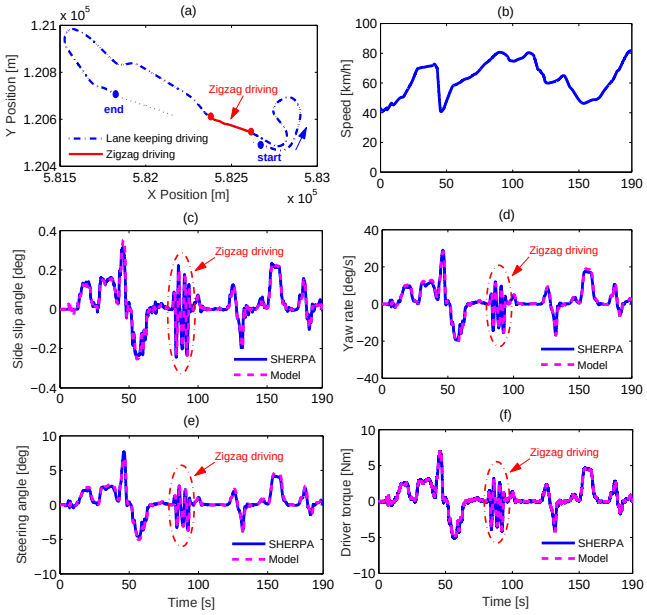

Fig. 9. Experimental validation of the driver-road-vehicle model obtained with the SHERPA simulator and the digital database of the Satory test track.

2) Scenario 3 [Wind Disturbance Rejection]: Assume that the vehicle is on a straight road with $v_x = 15$ [m/s] and subject to an important wind force $f_w = 1000$ [N], see Fig. 10 (a). This wind force generates a yaw moment disturbance which can be felt by the driver through the steering wheel. The disturbance rejection performance of the proposed control method is examined for three following cases:

- Case 1: full automatic control ($T_d = 0$),
- Case 2: manual control ($T_c = 0$),
- Case 3: driver-automation shared control.

Observe in Figs. 10 (b) and (c) that for all three cases, the required torques for disturbance rejection are similar and the

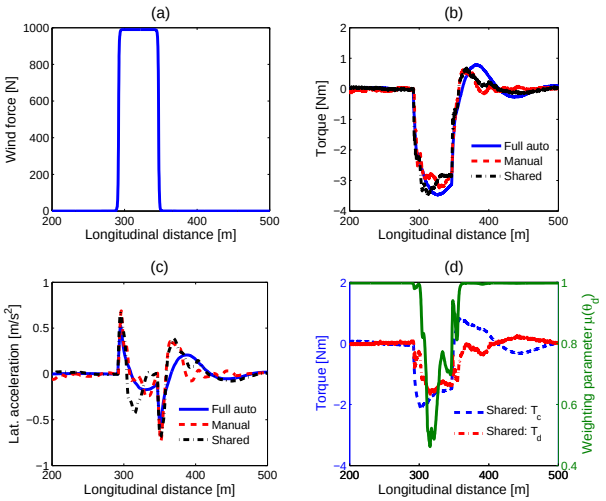

Fig. 10. Disturbance rejection performance for three cases: (1) full automatic control, (2) manual control, (3) shared control.

lateral accelerations remain small. In particular, for Case 3 the assistance torque T_c is in accordance with the driver's need for assistance (represented by $\mu(\theta_d)$) to help the driver. Thus, both driving actors *jointly* control the vehicle (i.e. their torques have the same sign) and the driver provides a smaller effort than that of Case 2 to perform the same task, see Fig. 10 (d).

Fig. 11 shows the comparison of the vehicle responses obtained with three above cases. As can be seen, the closed-loop behaviors of these cases are quite close. However, with the proposed shared controller (Case 3), the driver only needs to provide about half amount of the required torque for disturbance rejection, see Fig. 10 (d). This is particularly useful not only to improve the driving comfort but also to ensure the security in cases where the driver (for some reasons such as illness, inattention, etc.) cannot provide enough effort for the driving task. Observe also in Fig. 11 that the wind disturbance is effectively rejected for all three cases since all tracking performance variables remain small during the test.

To further point out the interest of the $\mathcal{H}_\infty$ performance in terms of disturbance rejection, let us compare the control performance obtained with full automatic control ($T_d = 0$) for two cases: *with* and *without* consideration of (15) in the control design presented in Theorem 2. As expected, Fig. 12 shows a clear improvement (i.e. smaller tracking errors under the effect of the wind disturbance) when the $\mathcal{H}_\infty$ performance is *explicitly* taken into account in the synthesis procedure.

3) Scenario 4 [Driver Monitoring for Shared Control]: This test aims to show the crucial role of the driver monitoring in the proposed shared control method. To this end, the lane keeping is performed in *shared control* mode (i.e. both the human driver and the proposed shared controller are involved in the driving task) over a section of the Satory test track, see Fig. 13 (a). The corresponding vehicle speed is depicted in Fig. 13 (e). This test scenario can be divided into two phases. For the first phase (from $t = 0s$ to $t = 45s$), the driver is assumed to be fully aware of the driving situation with $DS = 1$ as indicated in Fig. 13 (c). As expected, both driving actors *jointly*

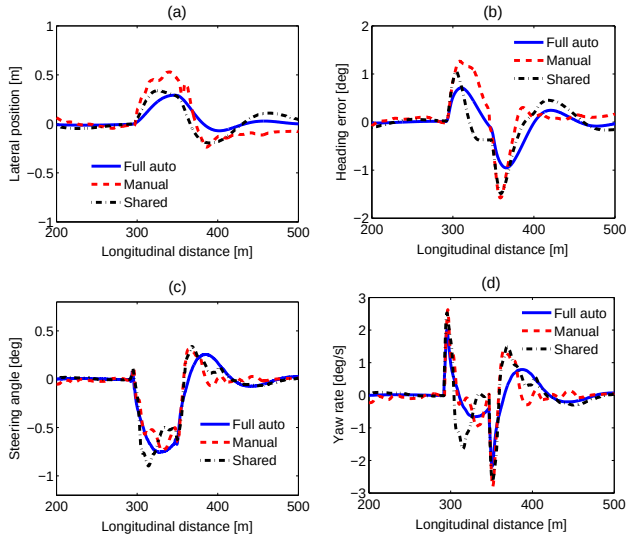

Fig. 11. Vehicle responses corresponding to the control results in Fig. 10.

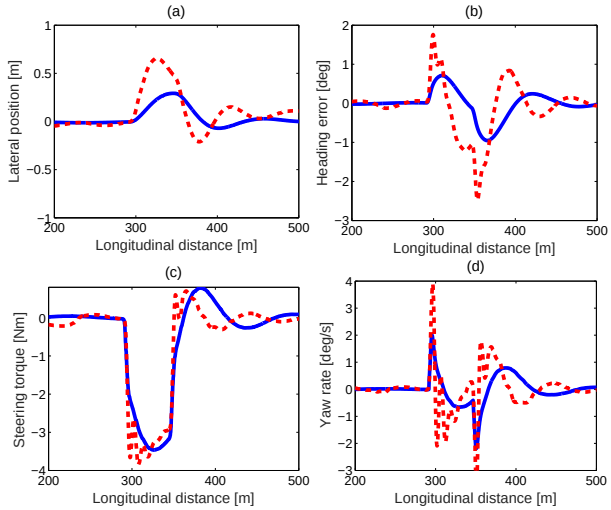

Fig. 12. Comparison of vehicle responses with respect to the wind force disturbance shown in Fig. 10 (a) for two cases: *with* (solid line) and *without* (dashed line) consideration of the $\mathcal{H}_\infty$ performance in the control design.

control the vehicle in this phase to perform different curve takings with different levels of assistance (according to the curve radius), see Figs. 13 (b) and (d). These experimental results also confirm those presented in Fig. 6 and indicate the usefulness of the simulation studies.

The second phase (from $t = 45s$ to $t = 75s$) corresponds to a lane keeping on a straight lane with the assumption that the driver is distracted ($DS = 0$), see Fig. 13 (c). For this, the driver did not watch the road (to simulate the distraction) while applying some torque on the steering wheel. As indicated in Fig. 13 (d), the maximal level of assistance is now required to realize the driving task with a "distracted" driver. As a consequence, the LKA system counteracts the driver's actions (i.e. their respective torques are in the opposite sign) to avoid the lane departure, see Fig. 13 (b). We can also observe in Figs. 13 (f), (g), and (h) that during the driving Scenario 4, the vehicle is maintained in the lane despite the driver's distraction in the second phase and the tracking performance variables remain small over the whole driving test.

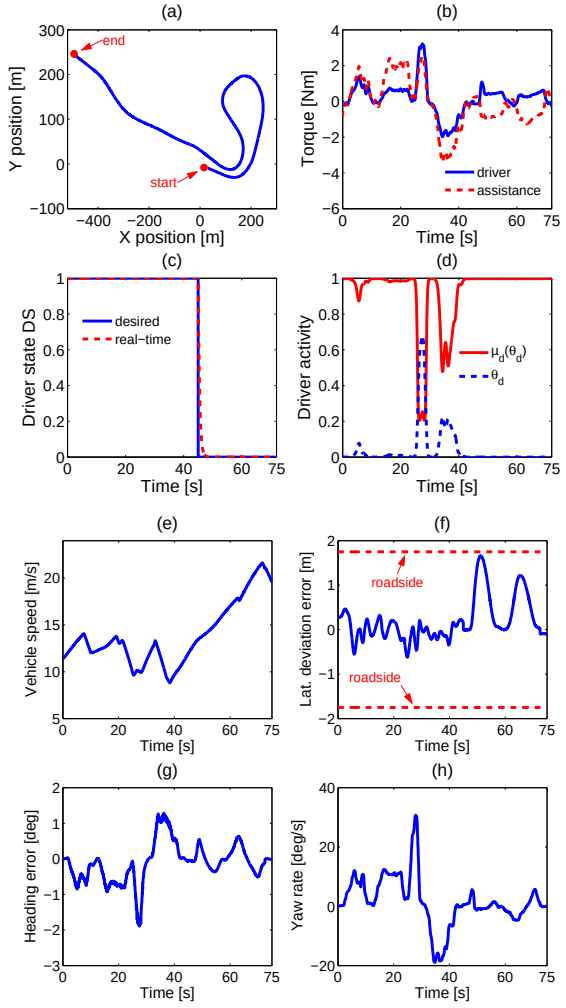

Fig. 13. Lane keeping performance over a road section of the Satory test track in accordance with the influence of the driver monitoring.

The above numerical and experimental results point out the effectiveness of the new shared control method under various driving circumstances despite the *unavailability* of two important vehicle sensors for lateral speed and steering rate.

VI. Concluding Remarks

An adaptive control authority allocation approach has been proposed to deal with the shared steering control between a human driver and a LKA system. To this end, a measured variable representing the real-time driving activity of the driver has been judiciously introduced into the driver-road-vehicle system. As a result, the designed actions of the LKA system can be computed in accordance with the driver's behaviors and the challenging driver-automation interaction is effectively managed. T-S fuzzy model-based control has been used to handle the *time-varying* nature of the driver activity variable and the vehicle speed. In particular, the proposed solution is cost-effective in the sense that a fuzzy output feedback control scheme is exploited to reduce two important vehicle sensors.

These latter have been intensively used in previous works for the control design and real-time implementation although they are not always available in commercial vehicles. The effectiveness of the proposed control methodology has been clearly demonstrated through both numerical and hardware experiments with different driving situations. Future works focus on the intensive human-factor experiments with a large panel of drivers and different real-world driving conditions to further evaluate the new shared control methodology for the LKA systems of intelligent vehicles.

REFERENCES

[1] J. Navarro, F. Mars, and M. Young, "Lateral control assistance in car driving: Classification, review and future prospects," *IET Intel. Transport Syst.*, vol. 5, no. 3, pp. 207–220, June 2011.

[2] D. Katzourakis, N. Lazic, and M. Lidberg, "Driver steering override for lane-keeping aid using computer-aided engineering," *IEEE/ASME Trans. Mechatron.*, vol. 20, no. 4, pp. 1543–1552, Aug. 2015.

[3] L. Li, D. Wen, N.-N. Zheng, and L.-C. Shen, "Cognitive cars: A new frontier for ADAS research," *IEEE Trans. Intell. Transp. Syst.*, vol. 13, no. 1, pp. 395–407, Mar. 2012.

[4] L. Saleh, P. Chevrel, F. Claveau, J.-F. Lafay, and F. Mars, "Shared steering control between a driver and an automation: Stability in the presence of driver behavior uncertainty," *IEEE Trans. Intell. Transp. Syst.*, vol. 14, no. 2, pp. 974–983, Mar. 2013.

[5] A.-T. Nguyen, C. Sentouh, and J.-C. Popieul, "Driver-automation cooperative approach for shared steering control under multiple system constraints: Design and experiments," *IEEE Trans. Ind. Electron.*, vol. PP, no. 99, pp. 1–1, Dec. 2016, doi: 10.1109/TIE.2016.2645146.

[6] S. M. Erlien, S. Fujita, and J. C. Gerdes, "Shared steering control using safe envelopes for obstacle avoidance and vehicle stability," *IEEE Trans. Intell. Transp. Syst.*, vol. 17, no. 2, pp. 441–451, Feb. 2016.

[7] D. A. Abbink, M. Mulder, and E. R. Boer, "Haptic shared control: smoothly shifting control authority?" *Cogn. Technol. Work*, vol. 14, no. 1, pp. 19–28, Nov. 2012.

[8] M. Johns, B. Mok, D. Sirkin, N. Gowda, C. Smith, W. Talamonti, and W. Ju, "Exploring shared control in automated driving," in *11th ACM/IEEE Int. Conf. Human-Robot Interact.*, Mar. 2016, pp. 91–98.

[9] F. Flemisch, F. Nashashibi, N. Rauch, A. Schieben, S. Glaser, G. Temme, P. Resende *et al.*, "Towards highly automated driving: Intermediate report on the HAVEit-joint system," in *3rd European Road Transport Research Arena*, Brussels, Belgium, June 2010.

[10] B. Soualmi, C. Sentouh, J. Popieul, and S. Debernard, "Automation-driver cooperative driving in presence of undetected obstacles," *Control Eng. Pract.*, vol. 24, pp. 106–119, Mar. 2014.

[11] K. Tanaka and H. Wang, *Fuzzy Control Systems Design and Analysis: a Linear Matrix Inequality Approach*. John Wiley & Sons, 2004.

[12] S. Yin, H. Gao, J. Qiu, and O. Kaynak, "Adaptive fault-tolerant control for nonlinear system with unknown control directions based on fuzzy approximation," *IEEE Trans. Syst. Man Cybern.: Syst.*, vol. PP, no. 99, pp. 1–10, May 2016, doi: 10.1109/TSMC.2016.2564921.

[13] A.-T. Nguyen, M. Sugeno, V. Campos, and M. Dambrine, "LMI-based stability analysis for piecewise multi-affine systems," *IEEE Trans. Fuzzy Syst.*, vol. PP, no. 99, pp. 1–1, May 2016, doi: 10.1109/TFUZZ.2016.2566798.

[14] S. Yin, P. Shi, and H. Yang, "Adaptive fuzzy control of strict-feedback nonlinear time-delay systems with unmodeled dynamics," *IEEE Trans. Cybern.*, vol. 46, no. 8, pp. 1926–1938, Aug. 2016.

[15] S. Boyd, L. El Ghaoui, E. Feron, and V. Balakrishnan, *Linear Matrix Inequalities in System and Control Theory*. Philadelphia: SIAM, 1994.

[16] A.-T. Nguyen, M. Dambrine, and J. Lauber, "Lyapunov-based robust control design for a class of switching non-linear systems subject to input saturation: application to engine control," *IET Control Theory Appl.*, vol. 8, no. 17, pp. 1789–1802, June 2014.

[17] S. Yin and Z. Huang, "Performance monitoring for vehicle suspension system via fuzzy positivistic C-means clustering based on accelerometer measurements," *IEEE/ASME Trans. Mechatron.*, vol. 20, no. 5, pp. 2613–2620, Oct. 2015.

[18] A.-T. Nguyen, C. Sentouh, and J.-C. Popieul, "Online adaptation of the authority level for shared lateral control of driver steering assist system using dynamic output feedback controller," in *41st Annu. Conf. IEEE Ind. Electron. Soc.*, Yokohama, Japan, Nov. 2015, pp. 3767–3772.

[19] R. Rajamani, *Vehicle Dynamics and Control*. Boston, Springer, 2012.

[20] D. D. Salvucci and R. Gray, "A two-point visual control model of steering," *Perception*, vol. 33, no. 10, pp. 1233–1248, Dec. 2004.

[21] C. Sentouh, B. Soualmi, J.-C. Popieul, and S. Debernard, "Cooperative steering assist control system," in *IEEE Int. Conf. on Syst., Man, and Cybern.*, Manchester, UK, Oct. 2013, pp. 941–946.

[22] Y. Dong, Z. Hu, K. Uchimura, and N. Murayama, "Driver inattention monitoring system for intelligent vehicles: A review," *IEEE Trans. Intell. Transp. Syst.*, vol. 12, no. 2, pp. 596–614, Dec. 2011.

[23] K.-Y. Lian, C.-H. Chiang, and H.-W. Tu, "LMI-based sensorless control of permanent-magnet synchronous motors," *IEEE Trans. Ind. Electron.*, vol. 54, no. 5, pp. 2769–2778, Oct. 2007.

[24] C. Scherer, P. Gahinet, and M. Chilali, "Multiobjective output-feedback control via LMI optimization," *IEEE Trans. Autom. Control*, vol. 42, no. 7, pp. 896–911, July 1997.

[25] H. Tuan, P. Apkarian, T. Narikiyo, and Y. Yamamoto, "Parameterized linear matrix inequality techniques in fuzzy control system design," *IEEE Trans. Fuzzy Syst.*, vol. 9, no. 2, pp. 324–332, Aug. 2001.

[26] J. Löfberg, "YALMIP: A toolbox for modeling and optimization in MATLAB," in *IEEE Int. Symp. on Comput. Aided Control Syst. Des.*, Taipei, Sept. 2004, pp. 284–289.

[27] C. Sentouh, P. Chevrel, F. Mars, and F. Claveau, "A sensorimotor driver model for steering control," in *IEEE Int. Conf. Syst., Man and Cybern.*, San Antonio, Texas, USA, Oct. 2009, pp. 2462–2467.

Anh-Tu Nguyen received Engineering and MSc degrees in 2009 from Grenoble Institute of Technology, France, and PhD degree in Automatic Control in 2013 from the University of Valenciennes, France.

After working a short period in 2010 at the French Institute of Petroleum, Dr. Nguyen began his doctoral program at the CNRS laboratory LAMIH in collaboration with VALEO Group. He was a postdoctoral researcher at the same laboratory from February 2014 to May 2016. Sine June 2016, he is a postdoctoral researcher at the CNRS laboratory LS2N. His research interests include robust control, constrained control systems, human-machine shared control for intelligent vehicles.

Chouki Sentouh received the MSc degree from the University of Versailles, France in 2003 and his PhD degree in Automatic Control from the University of Évry, France, in 2007.

Dr. Sentouh was a postdoctoral researcher at the CNRS laboratory IRCCyN, France, from 2007 to 2009. Since 2009, he is an Associate Professor at the University of Valenciennes in LAMIH-UMR CNRS 8201. His research fields include automotive control, driver assistance systems with driver interaction, human driver modeling and cooperation in intelligent transportation systems, shared control for assistance systems.

Jean-Christophe Popieul is Professor in Automatic Control at the University of Valenciennes in LAMIH-UMR CNRS 8201. Since 1994 his main area of interest is in Transport Safety. He first focused on driver status assessment and led several studies dealing with driver vigilance and workload in collaboration with automakers and insurance companies. In 2004 he started to work on ADAS. Beginning with longitudinal driver assistance, he is now working on control sharing for full driving automation. Specialized in Human Centered Automation, he is a member of several scientific boards, including ANR, PREDIT, i-Trans competitivity cluster, IRT Railenium. He is also the head of several Interactive Simulation Platforms of the LAMIH: SHERPA driving simulator, PSCHITT-Rail train/tramway simulator and PSCHITT-PMR wheelchair simulator.